Journal of Materials Chemistry C

ROYAL SOCIETY OF CHEMISTRY

PAPER

View Article Online
View Journal | View Issue

Cite this: J. Mater. Chem. C, 2022, 10, 2616

Diketopyrrolopyrrole-based conjugated polymers synthesized by direct arylation polycondensation for anisole-processed high mobility organic thin-film transistors†

Ying Sui,[ab] Zhongli Wang,[a] Junhua Bai,[a] Yibo Shi,[a] Xuwen Zhang,[a] Yunfeng Deng, *[a] Yang Han[a] and Yanhou Geng *[ac]

Received 5th September 2021,
Accepted 7th October 2021

DOI: 10.1039/d1tc04207f

rsc.li/materials-c

Two conjugated polymers (CPs) **Fu-F** and **Fu-Cl** that are soluble in a green solvent anisole were successfully synthesized *via* direct arylation polycondensation (DArP) using a furan-flanked diketopyrrolopyrrole (DPP) derivative (FDPP-Br) as the C–Br monomer and (*E*)-1,2-bis(3,4-difluorothien-2-yl)ethene (4FTVT) or (*E*)-1,2-bis(3,4-dichlorothien-2-yl)ethene (4ClTVT) as the C–H monomer. With anisole as the processing solvent and polyethylenimine ethoxylated (PEIE) as the electrode modification layer, n-type organic thin-film transistors (OTFTs) of the polymers were fabricated *via* bar-coating. The electron mobility (μ_e) of the devices based on **Fu-Cl** was only in the magnitude of 10^{-2} cm^2 V^{-1} s^{-1}, owing to the unfavoured fine granular film morphology. In contrast, **Fu-F** films showed fibre-like morphology with the polymer chains aligned along the bar-coating direction, which is favourable for the charge transport in OTFTs. Therefore, **Fu-F** delivered much better device performance with the μ_e of up to 2.79 cm^2 V^{-1} s^{-1}. Our study demonstrates that green solvent processed high mobility CPs can be synthesized by DArP, an emerging eco-friendly protocol for the synthesis of CPs.

1. Introduction

Conjugated polymer (CP)-based organic thin-film transistors (OTFTs) have received a lot of attention due to their intrinsic advantages of solution processability and mechanical flexibility.[1–8] Significant progress in material exploration and device engineering has pushed the performance of OTFTs of up to the commercialization threshold.[9–16] To date, halogenated solvents, such as chlorobenzene, *o*-dichlorobenzene (*o*-DCB), chloroform and so on, have usually been used for the fabrication of high performance OTFTs. These solvents suffer from serious health and environmental issues.[17–21] Therefore, the quest for high mobility CPs processible with green solvents is a matter of intense research.[17,18,22,23]

Diketopyrrolopyrrole (DPP)-based CPs represent one class of high mobility CPs that have been investigated the most in the past years.[24–26] In the above context, some DPP-based high mobility CPs processible with non-halogenated solvents, such as toluene, xylene, tetralin and tetrahydrofuran (THF), were also reported.[27–38] Lowering the regularity is generally adopted as an effective method to enhance the solubility of CPs.[27–29,39] For instance, Li *et al.* reported toluene-processed DPP-based high mobility CPs with decreased regioregularity.[28] Kwon *et al.* also demonstrated a DPP-based random copolymer for tetralin-processed OTFTs with a hole mobility (μ_h) of up to 6.05 cm^2 V^{-1} s^{-1}.[29] DPP-based CPs soluble in non-chlorinated solvents such as toluene, THF and hexane have also been demonstrated by incorporating furan into conjugated backbones.[39–41] Recently, we found that the solubility of DPP-based CPs could be remarkably enhanced by enriching the density of alkyl side chains, and accordingly poly(diketopyrrolopyrrole-*alt*-terchalcogenophene)s were soluble in non-chlorinated solvent *o*-xylene.[42,43] As a result, OTFTs with the μ_h of around 10 cm^2 V^{-1} s^{-1} were fabricated *via* bar-coating with *o*-xylene as the processing solvent.[43] In addition, the poly(diketopyrrolopyrrole-*alt*-terchalcogenophene)s based on furan-flanked DPP (FDPP) are even soluble in anisole, which is a green solvent according to the CHEM21 and Sanofi's solvent selection guides[44,45] and is used as the fragrance for cosmetics and as the additive for foods. OTFTs with a μ_h of up to 3.5 cm^2 V^{-1} s^{-1} were prepared with this solvent.[43] Note that the O···H non-covalent intramolecular interactions also occur in FDPP,[46] which is beneficial for the synthesis of high mobility CPs.

[a] School of Materials Science and Engineering and Tianjin Key Laboratory of Molecular Optoelectronic Science, Tianjin University, Tianjin 300072, P. R. China. E-mail: yunfeng.deng@tju.edu.cn, yanhou.geng@tju.edu.cn
[b] School of Materials Science and Engineering, Tianjin Chengjian University, Tianjin 300384, P. R. China
[c] Joint School of National University of Singapore and Tianjin University, International Campus of Tianjin University, Fuzhou 350207, China

† Electronic supplementary information (ESI) available. See DOI: 10.1039/d1tc04207f

Besides high mobility CPs processed using eco-friendly solvents, other aspects, such as material synthesis/purification and all steps of device fabrication, are expected to be green in the future applications of OTFTs. In this regard, environmentally benign and atom-economical protocols for the synthesis of high mobility CPs are also highly desired. At present, high mobility CPs are mainly prepared by Pd-catalysed Stille or Suzuki polycondensation, which need high-purity organometallic reagents prepared using tedious steps. Moreover, the organotin wastes produced in Stille polycondensation are highly toxic.[47–49] By contrast, direct arylation polycondensation (DArP) invokes C–H bond activation in the selected monomer through concerted metalation–deprotonation (CMD) instead of transmetalation, which reduces the synthetic steps of monomers and the production of toxic byproducts.[50–55] Therefore, DArP is recognized as an emerging protocol for the environmentally benign and atom-economical synthesis of CPs.[50–57]

Based on the above discussion, it is desirable to synthesize green solvent processible high mobility CPs *via* DArP. In the current paper, we selected a FDPP derivative as the C–Br monomer to conduct DArP with two highly reactive C–H monomers, *i.e.*, (*E*)-1,2-bis(3,4-difluorothien-2-yl)ethene (4FTVT)[58–60] and (*E*)-1,2-bis(3,4-dichlorothien-2-yl)-ethene (4ClTVT).[61] Two CPs, named **Fu-F** and **Fu-Cl**, that are soluble in *o*-xylene and anisole were successfully synthesized (Scheme 1). Top-gate/bottom-contact (TGBC) OTFTs with a reliable electron mobility (μ_e) of up to 2.79 $cm^2\ V^{-1}\ s^{-1}$ have been fabricated with anisole as the solvent. To the best of our knowledge, this has been the highest electron mobility reported so far for the real green solvent processed n-type OTFTs. Our study, for the first time, offers high mobility CPs that are synthesized *via* an environmentally benign protocol DArP and meanwhile can be processed using a green solvent.

2. Results and discussion

2.1. Synthesis and characterization

The synthetic route to the polymers **Fu-F** and **Fu-Cl** is depicted in Scheme 1 and the details of synthesis are summarized in the (ESI†). 4FTVT, 4ClTVT and 3,6-bis(5-bromofuran-2-yl)-2,5-bis(4-tetradecyloctadecyl)-pyrrolo[3,4-*c*]pyrrole-1,4(2*H*,5*H*)-dione (FDPP-Br) were prepared according to previous studies.[43,58,61] DArP was conducted following our previously reported procedure by using toluene as the solvent.[58,61] The resulting **Fu-F** and **Fu-Cl** were purified by precipitation in methanol and Soxhlet extraction with ethanol, acetone and hexane in succession. The molecular weights of the polymers were determined by high-temperature gel permeation chromatography (HT-GPC) at 150 °C using 1,2,4-trichlorobenzene (TCB) as the eluent and polystyrene (PS) as the standard. The number-average molecular weights (M_ns) of **Fu-F** and **Fu-Cl** are 37.2 and 63.0 kDa, respectively, with the corresponding polydispersity indices (*Đ*) of 2.1 and 2.3. The thermal properties of the two polymers were characterized by thermogravimetric analysis (TGA) and differential scanning calorimetry (DSC) under a nitrogen atmosphere. Both **Fu-F** and **Fu-Cl** exhibited excellent thermal stability with decomposition temperatures (T_d, 5% weight loss) of 415 and 407 °C, respectively (Fig. S1a, ESI†). As indicated by DSC scans (Fig. S1b, ESI†), there is no obvious thermal transition in the range of 25 to 300 °C for both polymers.

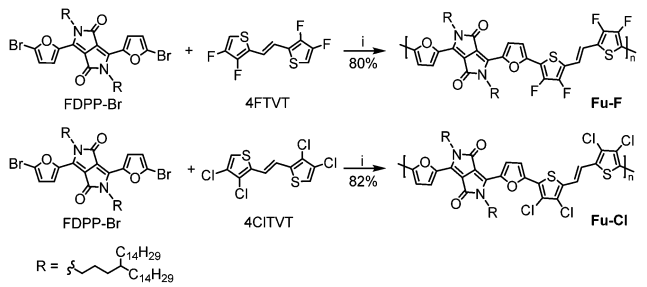

Scheme 1 Synthetic routes for the polymers. Reaction conditions: (i) Herrmann's cat., P(*o*-MeOPh)$_3$, PivOH, Cs_2CO_3, toluene, 120 °C.

The solubilities of **Fu-F** and **Fu-Cl** in *o*-DCB, *o*-xylene, and anisole that are ranked as hazardous, problematic, and recommended,[44,45,62,63] respectively, were investigated. As shown in Table S1 (ESI†), both polymers could be easily dissolved in *o*-xylene and *o*-DCB. They were also soluble in warm anisole with solubilities reaching 5 mg mL^{-1} at 70 °C, allowing the fabrication of OTFTs with anisole as the solvent. In contrast, analogous polymers based on thiophene-flanked DPP (TDPP), *i.e.*, **Th-F** and **Th-Cl**,[61,64] are almost insoluble in anisole (Table S1, ESI†). This observation is consistent with our previous study on poly(diketopyrrolopyrrole-*alt*-terchalcogenophene)s: introducing furan units at 3,6-positions of DPP can dramatically improve the solubilities of the DPP-based CPs.[43]

2.2. Optical and electrochemical properties

The solution absorption spectra of **Fu-F** and **Fu-Cl** in anisole, *o*-xylene and *o*-DCB and the absorption spectra of their thin films prepared using these three solvents were recorded (Fig. 1 and Fig. S2, ESI†), and the related data are summarized in Table 1 and Table S2 (ESI†). Both polymers show similar absorption features with two absorption bands, which is common to DPP-based CPs.[42,43,58,61,64] Solvent effect on the absorption spectra in both solution and film states is rather small. As shown in Table 1, the low energy absorption maxima (λ_{max}s) of **Fu-F** in three solvents are slightly different, which are at 797, 790 and 792 nm in anisole, *o*-xylene and *o*-DCB, respectively. A slightly red-shifted λ_{max} in anisole may be attributed to the stronger aggregation tendency of the polymer in this solvent.[65,66] The absorption spectra of the **Fu-F** pristine films prepared from these three solvents are almost overlapped (Fig. S2, ESI†), with 2–7 nm red-shifted λ_{max}s compared with those measured in solutions. The absorption spectra of the films before and after thermal annealing (200 °C for 10 min) are similar. **Fu-Cl** shows similar behaviour, but its λ_{max}s were red-shifted *ca.* 20 nm in solution and *ca.* 10 nm in film when compared with **Fu-F**. This phenomenon can be attributed to the stronger intramolecular charge transfer (ICT) of **Fu-Cl** originating from the larger dipole moment of the C–Cl bond.[67,68] The absorption spectra of **Fu-F** and **Fu-Cl** display *ca.* 30 nm blue-shifts compared with those of TDPP-based analogous polymers

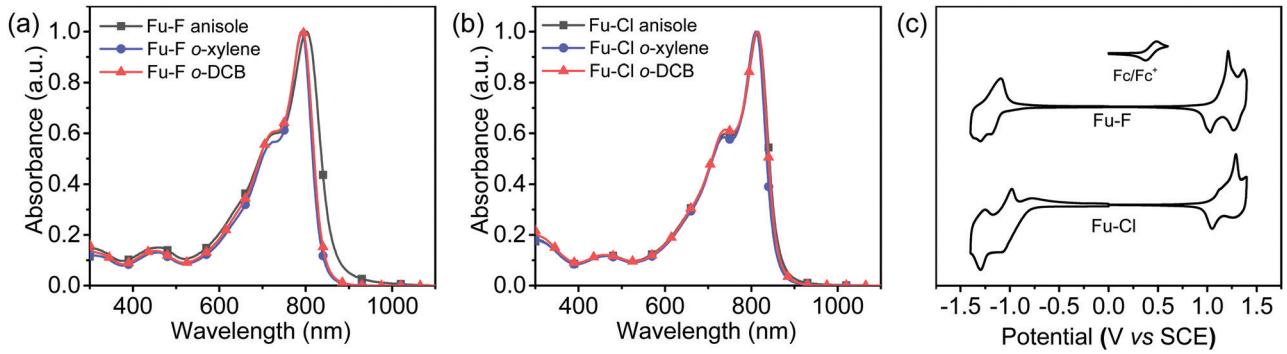

Fig. 1 Solution UV-vis-NIR absorption spectra of **Fu-F** (a) and **Fu-Cl** (b) and film cyclic voltammograms (CVs) (c) of the polymers. Solution spectra were measured in anisole, *o*-xylene and *o*-DCB with a concentration of 10^{-5} mol L^{-1} of the repeating units. Films for CV measurements were prepared by spin-coating the *o*-DCB solutions on working electrodes.

Table 1 Optical properties and energy levels of the polymers

	Anisole		*o*-Xylene		*o*-DCB			
Polymer	λ_{max}^{sol} (nm)	$\lambda_{max}^{film\ a}$ (nm)	λ_{max}^{sol} (nm)	$\lambda_{max}^{film\ a}$ (nm)	λ_{max}^{sol} (nm)	$\lambda_{max}^{film\ a}$ (nm)	$E_{onset}^{re}/E_{LUMO}{}^{b}$ (V/eV)	$E_{onset}^{ox}/E_{HOMO}{}^{b}$ (V/eV)
Fu-F	724, 797	719, 799	721, 790	713, 797	725, 792	713, 799	−0.84/−3.56	1.04/−5.44
Fu-Cl	741, 813	735, 810	736, 811	737, 811	744, 813	733, 814	−0.82/−3.58	1.05/−5.45

[a] The absorption maxima of pristine films without thermal annealing. [b] E_{LUMO} and E_{HOMO} calculated according to $E_{LUMO} = -(4.40 + E_{onset}^{re})$ eV and $E_{HOMO} = -(4.40 + E_{onset}^{ox})$ eV, in which E_{onset}^{re} and E_{onset}^{ox} represent reduction and oxidation onset potentials of the polymers *versus* SCE, respectively.

Th-F and **Th-Cl**,[61,64] ascribed to the effect of the size and electronegativity of the heteroatoms.

Film cyclic voltammograms (CVs) of the polymers (Fig. 1c) were recorded to estimate their highest occupied molecular orbital (HOMO) and lowest unoccupied molecular orbital (LUMO) energy levels. The redox onset potentials (E_{onset}^{re} and E_{onset}^{ox}) and calculated HOMO and LUMO energy levels (E_{HOMO} and E_{LUMO}) are summarized in Table 1. Both **Fu-F** and **Fu-Cl** exhibited quasi-reversible reduction and oxidation processes. The E_{HOMO}/E_{LUMO} values are −5.44/−3.56 eV for **Fu-F** and −5.45/−3.58 eV for **Fu-Cl**. **Fu-F** and **Fu-Cl** display deeper HOMO levels than **Th-F** and **Th-Cl**, which had the E_{HOMO} values of −5.34 and −5.41 eV, respectively, owing to the high ionization potential of furan.[69]

2.3. Charge transport properties

TGBC OTFTs were fabricated to evaluate the charge transport properties of the polymers. The semiconducting layer was deposited either by spin-coating or bar-coating followed by thermal annealing. The device performance was measured under ambient conditions, and the mobility values were extracted from the transfer characteristics in the saturation regime. The performance data of spin-coated and bar-coated OTFTs are summarized in Table S3 (ESI†) and Table 2, respectively.

First, OTFTs of **Fu-F** and **Fu-Cl** were prepared by spin-coating with anisole as the solvent and bare gold (Au) as source and drain electrodes. All devices exhibited electron-dominant ambipolar charge transport properties (Fig. S3 and S4, ESI†), consistent with the HOMO and LUMO energy levels of the polymers. The devices based on the semiconducting layers thermally annealed at 200 °C demonstrated the highest mobilities, with the maximum electron and hole mobilities ($\mu_{e,max}$ and $\mu_{h,max}$) of 1.30 and 0.36 $cm^2\ V^{-1}\ s^{-1}$ for **Fu-F** and 1.1×10^{-2} and 2.7×10^{-3} $cm^2\ V^{-1}\ s^{-1}$ for **Fu-Cl** (Table S3, ESI†).

Bar-coating is a printing technique suitable for the preparation of large area semiconducting layer in laboratory. Then, we fabricated OTFTs *via* bar-coating with anisole as the solvent. Fig. 2 shows the representative transfer and output curves of the bar-coated devices based on **Fu-F** and **Fu-Cl**, which are typical for ambipolar OTFTs. As shown in Table 2, bar-coated OTFTs of **Fu-F** with thermal annealing under optimized conditions (200 °C for 10 min) exhibited remarkably improved performance compared with spin-coated OTFTs, with $\mu_{e,max}$ and $\mu_{h,max}$ of 2.76 and 0.53 $cm^2\ V^{-1}\ s^{-1}$, respectively. However, the $\mu_{e,max}$ and $\mu_{h,max}$ of OTFTs based on **Fu-Cl** were only slightly enhanced to 1.3×10^{-2} and 3.5×10^{-3} $cm^2\ V^{-1}\ s^{-1}$, respectively. Bar-coated OTFTs of **Fu-F** were also fabricated with *o*-DCB and *o*-xylene as the solvents. The $\mu_{e,max}/\mu_{h,max}$ of the **Fu-F**-based devices processed with *o*-DCB and *o*-xylene were 2.23/0.73 and 1.07/0.43 $cm^2\ V^{-1}\ s^{-1}$, respectively. This indicates that green solvent can also deliver OTFTs with device performance superior to conventional chlorinated solvents. The above solvent dependence of device performance will be discussed thereinafter. Note that although a high μ_e was obtained, the threshold voltage (V_T) was rather high (Fig. 2 and Fig. S2–S6, ESI†) probably due to the parasitic resistance caused by the mismatch between the LUMO energy levels of the polymers and

Table 2 The performance of bar-coated OTFT devices of the polymers[a]

			Without modification						With PEIE modification		
			n-Channel			p-Channel			n-Channel		
Polymer	Solvent	T_A[b] (°C)	$\mu_{e,max}$[c] ($\mu_{e,avg}$[d]) ($cm^2 V^{-1} s^{-1}$)	V_T[e] (V)	I_{on}/I_{off}[f]	$\mu_{h,max}$[g] ($\mu_{h,avg}$[h]) ($cm^2 V^{-1} s^{-1}$)	V_T[e] (V)	I_{on}/I_{off}[f]	$\mu_{e,max}$[c] ($\mu_{e,avg}$[d]) ($cm^2 V^{-1} s^{-1}$)r[i] (%)	V_T[e] (V)	I_{on}/I_{off}[f]
Fu-F	Anisole	150	8.6×10^{-3} (7.5×10^{-3})	49–54	10^3–10^4	2.9×10^{-3} (2.1×10^{-3})	−30–−35	10^2–10^3			
		200	2.76 (2.42)	42–46	10^2–10^3	0.53 (0.41)	−48–−53	10^2–10^3	2.79 (2.48)78%	7–10	10^6–10^7
		250	1.03 (0.88)	50–55	10^3–10^4	0.34 (0.26)	−58–−61	10^3–10^4			
Fu-F	*o*-Xylene	200	1.07 (0.90)	51–55	10^3–10^4	0.43 (0.35)	−59–−63	10^4–10^5	0.70 (0.58)75%	7–11	10^6–10^7
Fu-F	*o*-DCB	200	2.23 (1.97)	48–54	10^3–10^4	0.73 (0.62)	−56–−60	10^3–10^4	2.21 (2.01)82%	8–13	10^3–10^4
Fu-Cl	Anisole	150	6.3×10^{-3} (5.1×10^{-3})	40–45	10^3–10^4	1.5×10^{-3} (1.0×10^{-3})	−30–−35	10^3–10^4			
		200	1.3×10^{-2} (9.9×10^{-3})	44–48	10^2–10^3	3.5×10^{-3} (2.5×10^{-3})	−45–−50	10^2–10^3	1.5×10^{-2} (1.1×10^{-2})77%	10–20	10^3–10^4
		250	3.6×10^{-3} (2.9×10^{-3})	45–50	10^3–10^4	2.9×10^{-3} (1.8×10^{-3})	−45–−49	10^3–10^4			

[a] The devices were measured under ambient conditions. [b] Thermal annealing temperature. [c] Maximum electron mobility calculated from the saturation regime. [d] Average electron mobility calculated from at least 15 devices. [e] Threshold voltage. [f] Current on/off ratio. [g] Maximum hole mobility calculated from the saturation regime. [h] Average hole mobility calculated from at least 15 devices. [i] Reliability factor.

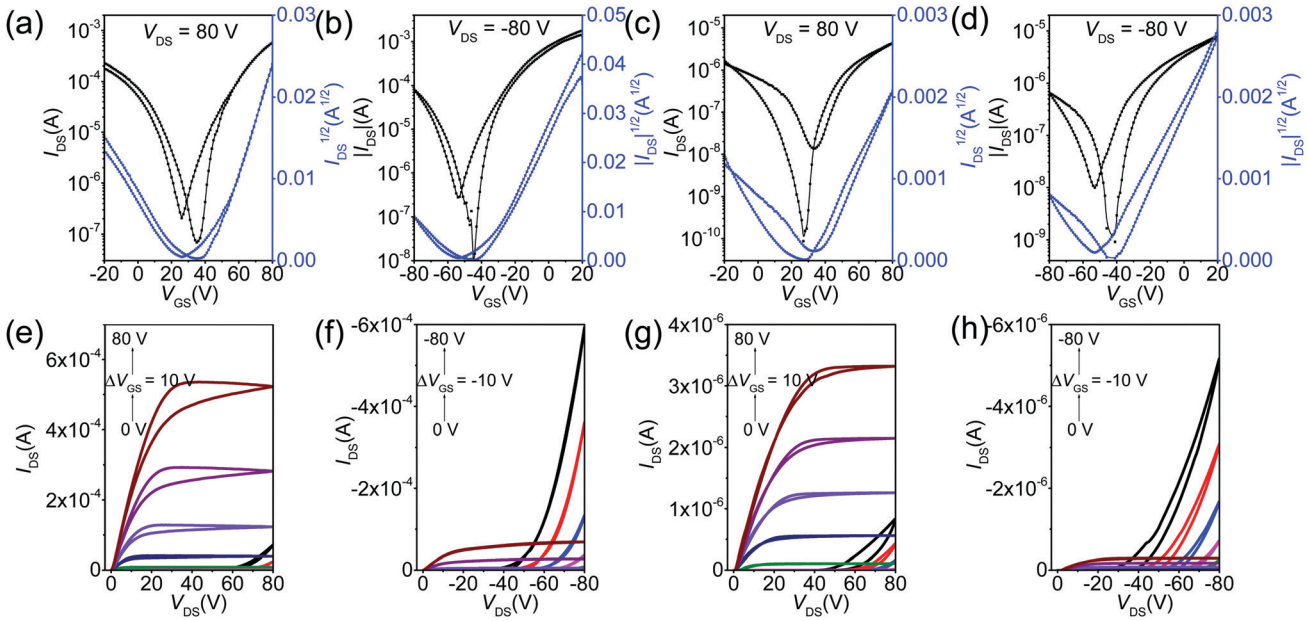

Fig. 2 Typical transfer (a–d) and output (e–h) curves of the OTFTs of **Fu-F** (a, b, e and f) and **Fu-Cl** (c, d, g and h) prepared by bar-coating. Thin films were prepared from anisole solutions on bare Si/SiO_2 substrates and annealed at 200 °C for 10 min in an inert atmosphere.

the work function of Au electrodes, resulting in non-ideal transistor behaviour.

To address the above issue, an ultrathin polyethylenimine ethoxylated (PEIE) layer was inserted between the Au electrodes and the polymer layer. The corresponding energy level diagrams are depicted in Fig. S7 (ESI†). It has been demonstrated that PEIE modification can effectively lower the work function of Au, and then facilitate efficient electron injection and block the hole injection from electrodes to the semiconducting layer.[70,71] Accordingly, all OTFTs with PEIE interlayer exhibited pure electron transport characteristics with much lower V_T (Fig. 3 and Fig. S8, S9, ESI†). As shown in Fig. 3c and d, obvious linear and saturation regions present in the output curves, and almost no hysteresis can be observed at different gate voltages (V_{GS}). Moreover, $(I_{DS})^{1/2}$ *versus* V_{GS} curves are linear with the absence of kinks. All these indicate that the devices operated in a near-ideal field-effect transistor mode. As shown in Table 2, bar-coated OTFTs of **Fu-F** with PEIE modification exhibited the $\mu_{e,max}$ of 2.79, 0.70 and 2.21 $cm^2 V^{-1} s^{-1}$, respectively, when anisole, *o*-xylene and *o*-DCB were used as processing solvents.

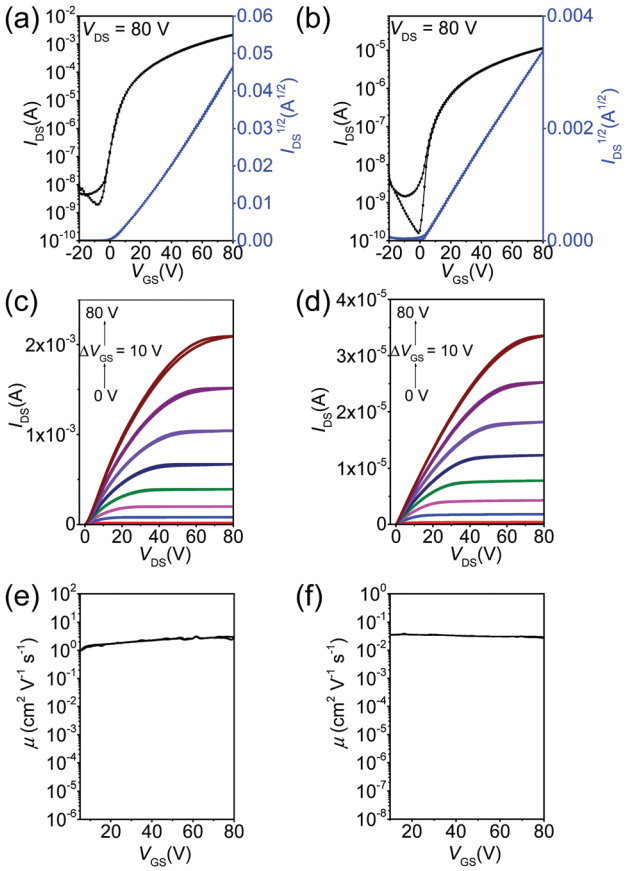

Fig. 3 Typical transfer (a and b), output (c and d) curves and saturation mobility *versus* V_{GS} (e and f) of OTFT devices based on **Fu-F** (a, c and e) and **Fu-Cl** (b, d and f) prepared *via* bar-coating. Thin films were prepared from anisole solution on 0.08 wt% PEIE-modified substrates and annealed at 200 °C for 10 min in an inert atmosphere.

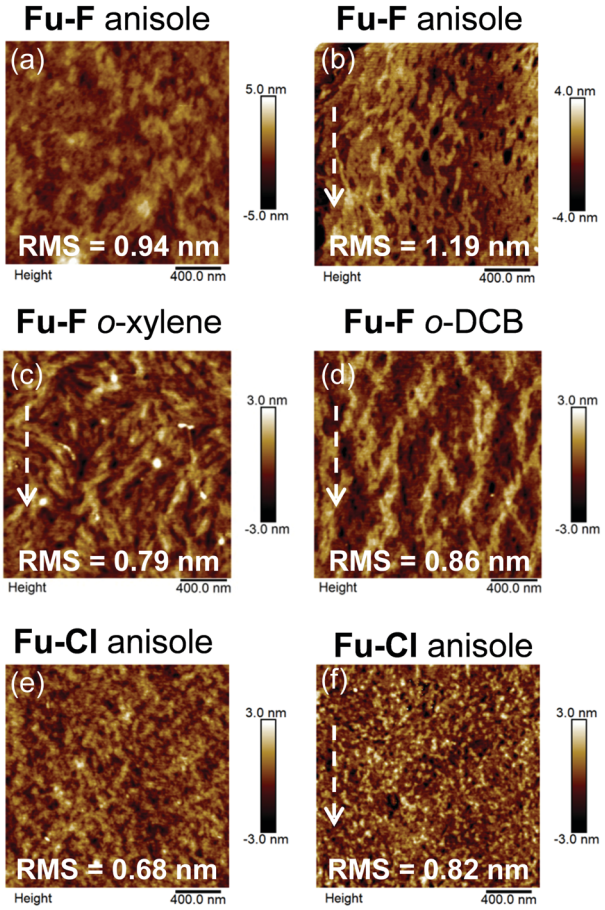

Fig. 4 AFM height images (2 μm × 2 μm) of the spin-coated (a and e) and bar-coated (b, c, d and f) polymer films from anisole, *o*-xylene and *o*-DCB solutions. Thin films were prepared on bare Si/SiO_2 substrates and annealed at 200 °C for 10 min under an inert atmosphere. The arrows in the images denote the bar-coating direction.

Bar-coated OTFTs of **Fu-Cl** with PEIE modification still showed inferior performance with a $\mu_{e,max}$ of 1.5 × 10^{-2} cm^2 V^{-1} s^{-1}, similar to the results observed in the OTFTs without the PEIE interlayer (Table 2). As shown in Fig. 3e and f, the electron mobility (μ_e) of the devices was almost independent of V_{GS}, indicating that the μ_e values are highly reliable.

2.4. Film morphology and microstructures

Fig. 4 shows the atomic force microscopy (AFM) height images of the spin- and bar-coated films of the polymers on bare Si/SiO_2 substrates. The bar-coated films of **Fu-F** from all three solvents exhibited a fibre-like morphology (Fig. 4b–d), while the short grains were observed in the film spin-cast from anisole (Fig. 4a). The fibre-like nanostructures were oriented along the bar-coating direction for the films processed with anisole and *o*-DCB, while the nanostructures distributed almost isotropically in the film prepared with *o*-xylene. The films of **Fu-Cl**, prepared by either spin-coating or bar-coating, featured a fine granular morphology. A similar film morphology was observed for both polymers on PEIE-modified substrates (Fig. S10, ESI†). All these observations are consistent with the OTFT performance of the polymers discussed above. **Fu-F** is characterized by a favourable film morphology and can form aligned films *via* bar-coating with both anisole and *o*-DCB as the solvents, giving rise to high mobility. In contrast, the fine granular morphology of **Fu-Cl** films is not beneficial to charge transport, and the OTFTs based on **Fu-Cl** thus exhibited low charge carrier mobility. The bar-coated polymer films were also characterized by X-ray diffraction (XRD) with the incident light parallel to the coating direction. As shown in Fig. S11 (ESI†), only a weak (100) peak was observed in the out-of-plane diffraction patterns for the films of **Fu-F** and **Fu-Cl**. This phenomenon indicates the almost amorphous nature of these two polymers and is consistent with their better solubility compared to TDPP counterparts **Th-F** and **Th-Cl**.

To further confirm the formation of aligned films of **Fu-F** with bar-coating, film absorption spectra under linearly polarized light were measured and the corresponding dichroic ratio (R) values were calculated (Fig. S12, ESI†). As expected, the R values of the **Fu-F** films bar-coated with anisole and *o*-DCB were 2.89 and 2.38, respectively. This implies that the polymer chains of **Fu-F** were aligned along the bar-coating direction. In contrast, all the **Fu-Cl** films and the film of **Fu-F** bar-coated

with *o*-xylene showed the *R* values close to 1, indicative of the isotropic nature of the films.

3. Conclusions

In summary, two FDPP-based CPs have been synthesized by DArP. The resulting CPs **Fu-F** and **Fu-Cl** can also be dissolved in a green solvent anisole, besides being soluble in *o*-xylene and *o*-DCB. **Fu-F** displayed a much higher mobility compared to **Fu-Cl**, mainly ascribed to the favourable film morphology of **Fu-F**. OTFTs of **Fu-F** processed with anisole exhibited a performance comparable to and better than that of the devices fabricated with *o*-DCB and *o*-xylene, respectively. With source/drain electrodes modified *via* a PEIE interlayer, n-type OTFTs of **Fu-F** with reliable μ_e values of up to 2.79 $cm^2 V^{-1} s^{-1}$, have been fabricated. This study demonstrates a high mobility CP that can be synthesized *via* an environmentally benign protocol (*i.e.*, DArP) and processed using the green solvent anisole, which is of significance for future commercialization of OTFTs. To further improve the device performance of green solvent processed CPs, the comprehensive design of side chains and conjugated backbones based on the deep understanding on the solution aggregation behaviour of CPs in different organic solvents is highly desired.

Conflicts of interest

There are no conflicts to declare.

Acknowledgements

This work is supported by the National Natural Science Foundation of China (no. 51933008) and the Tianjin Natural Science Foundation (no. 19JCYBJC18100).

Notes and references

1 X. Guo, A. Facchetti and T. J. Marks, *Chem. Rev.*, 2014, **114**, 8943–9021.
2 S. Holliday, J. E. Donaghey and I. McCulloch, *Chem. Mater.*, 2013, **26**, 647–663.
3 Z. Liu, G. Zhang and D. Zhang, *Acc. Chem. Res.*, 2018, **51**, 1422–1432.
4 H. Sirringhaus, *Adv. Mater.*, 2014, **26**, 1319–1335.
5 S. Yuvaraja, A. Nawaz, Q. Liu, D. Dubal, S. G. Surya, K. N. Salama and P. Sonar, *Chem. Soc. Rev.*, 2020, **49**, 3423–3460.
6 F. Huang, Z. Bo, Y. Geng, X. Wang, L. Wang, Y. Ma, J. Hou, W. Hu, J. Pei, H. Dong, S. Wang, Z. Li, Z. Shuai, Y. Li and Y. Cao, *Acta Polym. Sin.*, 2019, **50**, 988–1046.
7 Z. F. Yao, Q. Y. Li, H. T. Wu, Y. F. Ding, Z. Y. Wang, Y. Lu, J. Y. Wang and J. Pei, *SmartMat*, 2021, **2**, 378–387.
8 J. Ouyang, *SmartMat*, 2021, **2**, 263–285.
9 J. Y. Back, H. Yu, I. Song, I. Kang, H. Ahn, T. J. Shin, S.-K. Kwon, J. H. Oh and Y.-H. Kim, *Chem. Mater.*, 2015, **27**, 1732–1739.
10 G. Kim, S. J. Kang, G. K. Dutta, Y. K. Han, T. J. Shin, Y. Y. Noh and C. Yang, *J. Am. Chem. Soc.*, 2014, **136**, 9477–9483.
11 J. Lee, S. H. Kang, S. M. Lee, K. C. Lee, H. Yang, Y. Cho, D. Han, Y. Li, B. H. Lee and C. Yang, *Angew. Chem., Int. Ed.*, 2018, **57**, 13629–13634.
12 J. Li, Y. Zhao, H. S. Tan, Y. Guo, C. A. Di, G. Yu, Y. Liu, M. Lin, S. H. Lim, Y. Zhou, H. Su and B. S. Ong, *Sci. Rep.*, 2012, **2**, 754.
13 C. Luo, A. K. Kyaw, L. A. Perez, S. Patel, M. Wang, B. Grimm, G. C. Bazan, E. J. Kramer and A. J. Heeger, *Nano Lett.*, 2014, **14**, 2764–2771.
14 Y. Yang, Z. Liu, J. Chen, Z. Cai, Z. Wang, W. Chen, G. Zhang, X. Zhang, L. Chi and D. Zhang, *Adv. Sci.*, 2018, **5**, 1801497.
15 Y. Sui, Y. Deng, T. Du, Y. Shi and Y. Geng, *Mater. Chem. Front.*, 2019, **3**, 1932–1951.
16 J. Liu, L. Jiang, W. Hu, Y. Liu and D. Zhu, *Sci. China: Chem.*, 2019, **62**, 313–330.
17 F. Campana, C. Kim, A. Marrocchi and L. Vaccaro, *J. Mater. Chem. C*, 2020, **8**, 15027–15047.
18 J. Cho, S. H. Yu and D. S. Chung, *J. Mater. Chem. C*, 2017, **5**, 2745–2757.
19 Agency for Toxic Substances & Disease Registry. Toxicological Profile for Chloroform, 2021, https://www.atsdr.cdc.gov/ToxProfiles/tp.asp.
20 Agency for Toxic Substances & Disease Registry. Toxicological Profile for Chlorobenzene, 2021, https://www.atsdr.cdc.gov/ToxProfiles/tp.asp.
21 Agency for Toxic Substances & Disease Registry. Public Health Statement for Dichlorobenzenes, 2021, https://www.atsdr.cdc.gov/phs/phs.asp.
22 D. Ho, J. Lee, S. Park, Y. Park, K. Cho, F. Campana, D. Lanari, A. Facchetti, S. Seo, C. Kim, A. Marrocchi and L. Vaccaro, *J. Mater. Chem. C*, 2020, **8**, 5786–5794.
23 J. Lee, S. A. Park, S. U. Ryu, D. Chung, T. Park and S. Y. Son, *J. Mater. Chem. A*, 2020, **8**, 21455–21473.
24 Y. Yang, Z. Liu, G. Zhang, X. Zhang and D. Zhang, *Adv. Mater.*, 2019, **31**, e1903104.
25 C. B. Nielsen, M. Turbiez and I. McCulloch, *Adv. Mater.*, 2013, **25**, 1859–1880.
26 M. Kim, S. U. Ryu, S. A. Park, K. Choi, T. Kim, D. Chung and T. Park, *Adv. Funct. Mater.*, 2019, **30**, 1904545.
27 H. H. Choi, J. Y. Baek, E. Song, B. Kang, K. Cho, S. K. Kwon and Y. H. Kim, *Adv. Mater.*, 2015, **27**, 3626–3631.
28 Y. Ji, C. Xiao, Q. Wang, J. Zhang, C. Li, Y. Wu, Z. Wei, X. Zhan, W. Hu, Z. Wang, R. A. Janssen and W. Li, *Adv. Mater.*, 2016, **28**, 943–950.
29 H. J. Yun, G. B. Lee, D. S. Chung, Y. H. Kim and S. K. Kwon, *Adv. Mater.*, 2014, **26**, 6612–6616.
30 M. Lee, M. J. Kim, S. Ro, S. Choi, S. M. Jin, H. D. Nguyen, J. Yang, K. K. Lee, D. U. Lim, E. Lee, M. S. Kang, J. H. Choi, J. H. Cho and B. Kim, *ACS Appl. Mater. Interfaces*, 2017, **9**, 28817–28827.

31 W.-Y. Lee, G. Giri, Y. Diao, C. J. Tassone, J. R. Matthews, M. L. Sorensen, S. C. B. Mannsfeld, W.-C. Chen, H. H. Fong, J. B. H. Tok, M. F. Toney, M. He and Z. Bao, *Adv. Funct. Mater.*, 2014, **24**, 3524–3534.
32 J. R. Matthews, W. Niu, A. Tandia, A. L. Wallace, J. Hu, W.-Y. Lee, G. Giri, S. C. B. Mannsfeld, Y. Xie, S. Cai, H. H. Fong, Z. Bao and M. He, *Chem. Mater.*, 2013, **25**, 782–789.
33 B. Fu, C.-Y. Wang, B. D. Rose, Y. Jiang, M. Chang, P.-H. Chu, Z. Yuan, C. Fuentes-Hernandez, B. Kippelen, J.-L. Brédas, D. M. Collard and E. Reichmanis, *Chem. Mater.*, 2015, **27**, 2928–2937.
34 M. M. Dereje, D. Ji, S.-H. Kang, C. Yang and Y.-Y. Noh, *Dyes Pigm.*, 2017, **145**, 270–276.
35 I. Song, H.-W. Kim, J. Ahn, M. Han, S.-K. Kwon, Y.-H. Kim and J. H. Oh, *J. Mater. Chem. C*, 2019, **7**, 14977–14985.
36 H.-J. Yun, J. Cho, D. S. Chung, Y.-H. Kim and S.-K. Kwon, *Macromolecules*, 2014, **47**, 7030–7035.
37 G.-J. N. Wang, F. Molina-Lopez, H. Zhang, J. Xu, H.-C. Wu, J. Lopez, L. Shaw, J. Mun, Q. Zhang, S. Wang, A. Ehrlich and Z. Bao, *Macromolecules*, 2018, **51**, 4976–4985.
38 G. Feng, Y. Xu, C. Xiao, J. Zhang, X. Zhang, C. Li, Z. Wei, W. Hu, Z. Wang and W. Li, *Polym. Chem.*, 2016, **7**, 164–170.
39 S. Ding, Z. Ni, M. Hu, G. Qiu, J. Li, J. Ye, X. Zhang, F. Liu, H. Dong and W. Hu, *Macromol. Rapid Commun.*, 2018, **39**, e1800225.
40 P. Sonar, J. Chang, J. H. Kim, K. H. Ong, E. Gann, S. Manzhos, J. Wu and C. R. McNeill, *ACS Appl. Mater. Interfaces*, 2016, **8**, 24325–24330.
41 S. M. Lee, H. R. Lee, A. R. Han, J. Lee, J. H. Oh and C. Yang, *ACS Appl. Mater. Interfaces*, 2017, **9**, 15652–15661.
42 Z. Wang, X. Song, Y. Jiang, J. Zhang, X. Yu, Y. Deng, Y. Han, W. Hu and Y. Geng, *Adv. Sci.*, 2019, **6**, 1902412.
43 Z. Wang, Y. Shi, Y. Deng, Y. Han and Y. Geng, *Adv. Funct. Mater.*, 2021, 2104881.
44 D. Prat, A. Wells, J. Hayler, H. Sneddon, C. R. McElroy, S. Abou-Shehada and P. J. Dunn, *Green Chem.*, 2016, **18**, 288–296.
45 D. Prat, O. Pardigon, H.-W. Flemming, S. Letestu, V. Ducandas, P. Isnard, E. Guntrum, T. Senac, S. Ruisseau, P. Cruciani and P. Hosek, *Org. Process Res. Dev.*, 2013, **17**, 1517–1525.
46 C. Fu, F. Bélanger-Gariépy and D. F. Perepichka, *CrystEngComm*, 2016, **18**, 4285–4289.
47 J. R. Pouliot, F. Grenier, J. T. Blaskovits, S. Beaupre and M. Leclerc, *Chem. Rev.*, 2016, **116**, 14225–14274.
48 Y. Ran, Y. Guo and Y. Liu, *Mater. Horiz.*, 2020, **7**, 1955–1970.
49 Y. Geng and Y. Sui, *Acta Polym. Sin.*, 2019, **20**, 109–116.
50 T. Bura, S. Beaupre, M. A. Legare, J. Quinn, E. Rochette, J. T. Blaskovits, F. G. Fontaine, A. Pron, Y. Li and M. Leclerc, *Chem. Sci.*, 2017, **8**, 3913–3925.
51 N. S. Gobalasingham and B. C. Thompson, *Prog. Polym. Sci.*, 2018, **83**, 135–201.
52 A. Facchetti, L. Vaccaro and A. Marrocchi, *Angew. Chem., Int. Ed.*, 2012, **51**, 3520–3523.
53 M. Wakioka and F. Ozawa, *Asian J. Org. Chem.*, 2018, **7**, 1206–1216.
54 S. Phan and C. K. Luscombe, *Trends Chem.*, 2019, **1**, 670–681.
55 A. S. Dudnik, T. J. Aldrich, N. D. Eastham, R. P. Chang, A. Facchetti and T. J. Marks, *J. Am. Chem. Soc.*, 2016, **138**, 15699–15709.
56 Z. Ni, H. Wang, H. Dong, Y. Dang, Q. Zhao, X. Zhang and W. Hu, *Nat. Chem.*, 2019, **11**, 271–277.
57 X. Guo, Y. Zhang, Y. Hu, J. Yang, Y. Li, Z. Ni, H. Dong and W. Hu, *Angew. Chem., Int. Ed.*, 2021, **60**, 14902–14908.
58 Y. Gao, X. Zhang, H. Tian, J. Zhang, D. Yan, Y. Geng and F. Wang, *Adv. Mater.*, 2015, **27**, 6753–6759.
59 K. Guo, J. Bai, Y. Jiang, Z. Wang, Y. Sui, Y. Deng, Y. Han, H. Tian and Y. Geng, *Adv. Funct. Mater.*, 2018, **28**, 1801097.
60 K. Guo, Y. Jiang, Y. Sui, Y.-F. Deng and Y.-H. Geng, *Chin. J. Polym. Sci.*, 2019, **37**, 1099–1104.
61 Y. Sui, Y. Shi, Y. Deng, R. Li, J. Bai, Z. Wang, Y. Dang, Y. Han, N. Kirby, L. Ye and Y. Geng, *Macromolecules*, 2020, **53**, 10147–10154.
62 R. K. Henderson, C. Jiménez-González, D. J. C. Constable, S. R. Alston, G. G. A. Inglis, G. Fisher, J. Sherwood, S. P. Binks and A. D. Curzons, *Green Chem.*, 2011, **13**, 854–862.
63 C. M. Alder, J. D. Hayler, R. K. Henderson, A. M. Redman, L. Shukla, L. E. Shuster and H. F. Sneddon, *Green Chem.*, 2016, **18**, 3879–3890.
64 Y. Gao, J. Bai, Y. Sui, Y. Han, Y. Deng, H. Tian, Y. Geng and F. Wang, *Macromolecules*, 2018, **51**, 8752–8760.
65 B. Fan, L. Ying, Z. Wang, B. He, X.-F. Jiang, F. Huang and Y. Cao, *Energy Environ. Sci.*, 2017, **10**, 1243–1251.
66 Z. Wang, Z. Liu, L. Ning, M. Xiao, Y. Yi, Z. Cai, A. Sadhanala, G. Zhang, W. Chen, H. Sirringhaus and D. Zhang, *Chem. Mater.*, 2018, **30**, 3090–3100.
67 H. Zhang, H. Yao, J. Hou, J. Zhu, J. Zhang, W. Li, R. Yu, B. Gao, S. Zhang and J. Hou, *Adv. Mater.*, 2018, **30**, e1800613.
68 Q. Zhao, J. Qu and F. He, *Adv. Sci.*, 2020, **7**, 2000509.
69 D. Chandran, T. Marszalek, W. Zajaczkowski, P. K. Madathil, R. K. Vijayaraghavan, Y.-H. Koh, S.-Y. Park, J. R. Ochsmann, W. Pisula and K.-S. Lee, *Polymer*, 2015, **73**, 205–213.
70 J. Bai, Y. Jiang, Z. Wang, Y. Sui, Y. Deng, Y. Han and Y. Geng, *Adv. Electron. Mater.*, 2019, **6**, 1901002.
71 Y. Zhou, C. Fuentes-Hernandez, J. Shim, J. Meyer, A. J. Giordano, H. Li, P. Winget, T. Papadopoulos, H. Cheun, J. Kim, M. Fenoll, A. Dindar, W. Haske, E. Najafabadi, T. M. Khan, H. Sojoudi, S. Barlow, S. Graham, J.-L. Brédas, S. R. Marder, A. Kahn and B. Kippelen, *Science*, 2012, **336**, 317–332.

